AD-A080 872 FOREST PRODUCTS LAB MADISON WI F/G 11/12
STRENGTH OF WOOD BEAMS WITH END SPLITS.(U)
1979 J F MURPHY
UNCLASSIFIED FSRP-FPL-347 NL

END
DATE FILMED
3-80
DTIC

United States
Department of
Agriculture

Forest Service

**Forest
Products
Laboratory**

Research
Paper
FPL 347

1979

Strength of Wood Beams With End Splits

Abstract

A method of analysis for determining crack propagation loads on wood beams with end splits is presented. The method is based on (1) linear elastic orthotropic fracture mechanics concepts, (2) theory of complex variables, and (3) least squares boundary value collocation (BVC). Using this method, the critical stress intensity factor, ~~K_{IIc} of Douglas-fir beams with end splits~~ is determined, ~~to be 2,035 psi $\sqrt{\text{in.}}$~~ Also, a simple failure equation for end split beams is proposed.

Acknowledgment

The author is indebted to C. B. Norris and E. C. O. Erickson, who conducted the experimental studies reported herein in 1951. They reported their results in an unpublished report. Their results have been reevaluated in the light of fracture mechanics theory in the preparation of this paper.

United States Department of Agriculture

Forest Service

Forest Products Laboratory[1]

Research Paper FPL 347

1979

(6)

Strength of Wood Beams With End Splits.

By

(10) JOSEPH F. MURPHY Engineer

(9) Forest Service research paper,

(11) 1979 (12) 15

(14) FSRP-FPL-347

Introduction

In the grading of timber for beams it is useful to have a quantitative measure of the effect of end splits on the strength of such beams. The method presented gives a way of predicting when an end crack will propagate resulting in a loss of stiffness and strength. Linear elastic fracture mechanics has been applied successfully to predict brittle failure (crack propagation) in wood (2,8,14).[2] Although the title problem has been examined (2), this report uses a different method of solution and simplifies the results while investigating the effect of different orthotropic parameters.

Before proceeding, linear elastic fracture mechanics will be overviewed. The propagation of a planar crack can be described, in the most general case, by the combination of three independent modes as shown in figure 1. The first mode, or opening mode, has the crack surfaces move in a normal direction with respect to the surface planes. The second, sliding, or forward shear, mode has the surfaces move in their respective planes in the direction parallel to collinear crack propagation. The third, tearing, or transverse shear, mode has the surfaces moving in their respective planes but perpendicular to collinear crack propagation. The opening mode results from inplane (a plane perpendicular to the crack front) symmetric (symmetric about the plane between crack plane surfaces) loading while the sliding mode results from inplane skew-symmetric loading. The third mode results from out of or antiplane loading conditions (loading parallel to crack front).

The theoretical stresses (see fig. 2 for positive stresses) for a small region directly ahead of the crack (the crack surfaces coincident with the negative x, z half plane) for the three modes are reduced from Sih et al. (15):

Mode I	*Mode II*
$\sigma_x = K_I \beta_1 \beta_2 (2\pi x)^{-1/2}$	$\sigma_x = 0$
$\sigma_y = K_I (2\pi x)^{-1/2}$	$\sigma_y = 0$
$\tau_{xy} = 0$	$\tau_{xy} = K_{II} (2\pi x)^{-1/2}$

Mode III

$$\tau_{xz} = 0$$

$$\tau_{yz} = K_{III} (2\pi x)^{-1/2}$$

$$\sigma_z = 0$$

[1] Maintained at Madison, Wis., in cooperation with the University of Wisconsin.

[2] Underlined numbers in parentheses refer to literature cited at end of report.

141700

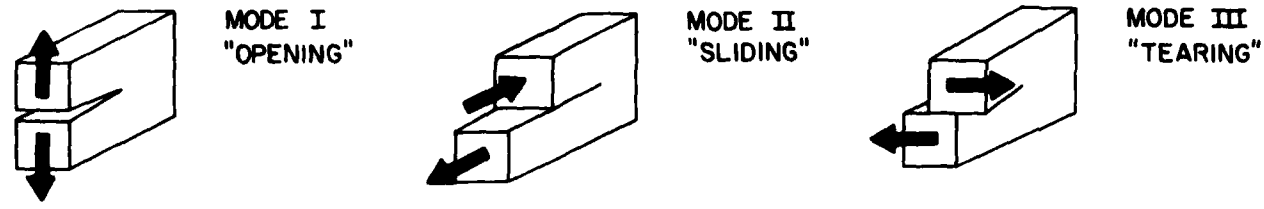

Figure 1.—Three basic modes of crack surface displacement.

(M 146 386)

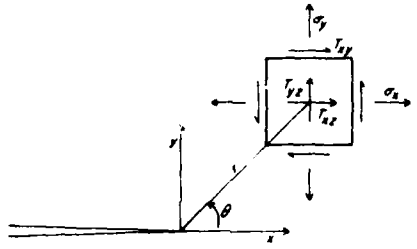

Figure 2.—Two-dimensional coordinate system around a crack tip with positive stresses.

(M 148 055)

where β_1, β_2 are orthotropic parameters, that is, the β's characterize the degree of orthotropy and are equal to one for isotropy (see appendix A), and the K's are stress intensity factors (SIF's) in I, II, or III loading modes.[3] The SIF's are linearly dependent on remote boundary conditions, strongly dependent on geometry, and weakly dependent on orthotropic parameters for finite bodies (the dependence on orthotropic parameters becomes stronger as the distance ahead of the crack and a free surface becomes smaller). In single-mode loading and collinear crack propagation, the crack propagates when the SIF reaches a critical value (K_{Ic}, K_{IIc}, or K_{IIIc}).

Theoretical Considerations

A boundary value collocation method was employed to solve for the theoretical SIF K_{II}. First a series solution was formulated which satisfies identically the field equation (a generalization of the biharmonic equation) and the stress-free condition on the crack surfaces (see appendix A). The unknown coefficients of the series solution were solved using boundary value collocation (see appendix B). Boundary values were resultant forces and moment (see eq. A5, A6). This method was employed because (1) after the coefficients are obtained, stresses and strains can be calculated anywhere in the body, (2) the first coefficient is linearly related to the SIF, (3) the set of linear equations result in a dense matrix requiring minimal computer storage space, and (4) more than one problem (different boundary values) can be solved simultaneously. The number of boundary points was increased until the SIF (first coefficient) converged, (e.g., in the concentrated load case, increasing the number of boundary points (each with three stress conditions) from 24 to 32 changed the SIF less than 0.8 pct). A more detailed description of the theoretical analysis is given in appendices A and B.

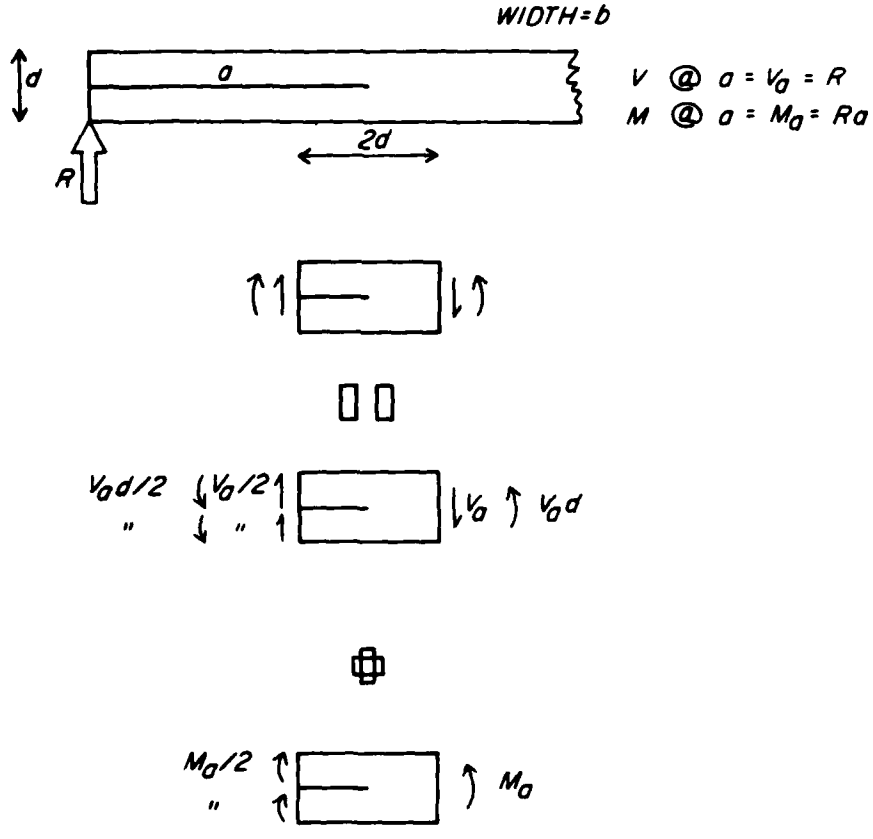

Figure 3.—End-split beam under concentrated load (superposition of two basic cases).

(M 148 056)

Theoretical Problem and Results

End-Split Beam Under A Concentrated Load

The problem considered is an end-split beam (end split horizontal, full width, and at middepth) as shown in figure 3. Assume no tractions on the

[3] Some authors use k_1, k_2, and k_3 as SIF's where $K_I = k_1\sqrt{\pi}$, $K_{II} = k_2\sqrt{\pi}$, and $K_{III} = k_3\sqrt{\pi}$.

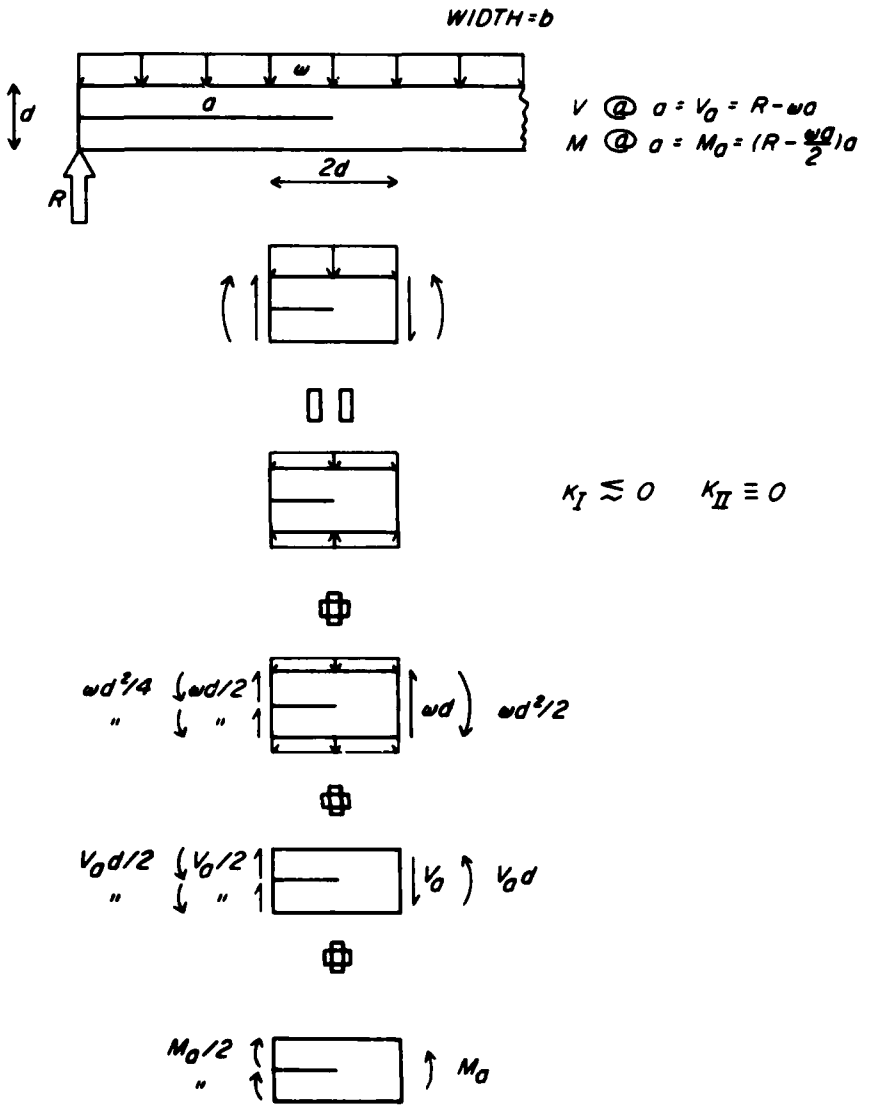

Figure 4.—End-split beam under uniform load (superposition of four basic cases).

(M 148 057)

surfaces of the split. The problem can be solved by superposing the solutions of two problems shown in figure 3. The two cases are solved and then the SIF can be written (using superposition):

$$K_{II} = A\frac{M}{bd^{3/2}} + B\frac{V}{bd^{1/2}} \qquad (1)$$

where the internal moment and shear, M and V, are calculated at the crack tip using elementary methods, A and B are constants dependent on the orthotropic parameters, and b and d are the beam width and depth, respectively.

End-Split Beam Under A Uniform Load

This problem is shown in figure 4 with subsequent breakdowns (again assume no crack surface tractions). The subcase with symmetric loading gives a negative opening mode SIF which would produce frictional forces between the two crack planes; therefore, as a conservative estimate, K_I will be taken as zero. As can be seen, only one more subcase is added than the concentrated load case. The K_{II} for a uniform load can then be estimated (conservatively) as:

$$K_{II} = A\frac{M}{bd^{3/2}} + B\frac{V}{bd^{1/2}} + C\frac{w}{bd^{-1/2}} \qquad (2)$$

where w is the uniform loading and C is a third constant dependent on the orthotropic parameters. Note equation (2) reduces to equation (1) for the concentrated load case (e.g., $w = 0$).

Effect of Different Orthotropic Parameters

Orthotropic parameters for different wood species and grain orientations and plane stress conditions are shown in figure 5 (see eq. (A2), (A3)). The coefficients A, B, and C (see eq. (2)) have been calculated for four extreme and one average combination of β_1 and β_2 shown in figure 5. The coefficients are given in table 1 and their respective concentrated load equations (eq. (1)) are plotted in figure 6. An equation to be used for any wood species and any grain orientation (constants have two significant figures) under concentrated or uniform load conditions is

$$K_{II} = -2.8\frac{M}{bd^{3/2}} - 0.72\frac{V}{bd^{1/2}} + 0.06\frac{w}{bd^{-1/2}}. \qquad (3)$$

Equation (3) is good (within 11 pct) for all β combinations in figure 6. Combined loading conditions can be considered by summing up the K_{II}'s for each loading condition yielding a total K_{II}. Failure occurs when absolute total K_{II} reaches a critical value, K_{IIc}. Therefore equation (3) with an appropriate K_{IIc} becomes a single failure criteria for end-split beams.

End-Split Beams Concentrated Load Experiments

The experimental data are from an unpublished report by C. B. Norris and E. C. O. Erickson, done in 1951. The following section is verbatim[4] from that report:

Description of Tests

"Two groups of substantially clear Douglas-fir beams (7.5- by 1.62-in.

[4] Figures, tables, and references are renumbered.

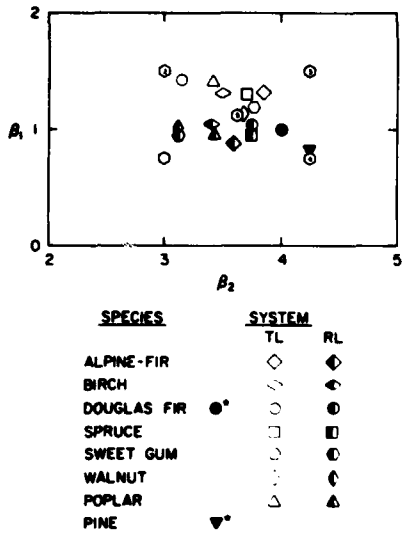

Figure 5.—Orthotropic parameters for different wood species for the TL, RL systems of crack propagation. (First letter refers to normal to crack planes or the y direction; the second letter refers to direction of crack propagation or the x direction.) Computed from elastic constants in (5) or *obtained from J. D. Barrett private communication.

(M 148 058)

cross section) were tested as shown in figure 7. Saw kerfs about 1/8-inch wide and of various lengths (see table 2) were cut at the centerline of the beams as shown in the figure. These kerfs were filled with smooth splines of wood which were well paraffined to reduce friction. The beams were supported on rockers and protected from indentation of the knife edges by steel plates 1-inch thick and extending 3 inches each side of the reaction in the direction of the length of the beams. The beams were laterally supported, near their ends, during test to keep them in a vertical plane. These supports did not hamper the deflection of the beams.

"Pillow blocks of hardwood were used to transfer the loads to the beams. For the beams of group 1, the pillow blocks were out to a 24-inch radius; and for the beams of group 2, to an 18-inch radius. The speed of the testing machine was 0.194 inch per minute for group 1 and 0.096 inch per minute for group 2. The deflections were measured to the nearest 0.01 inch at load increments varying from 200 to 500 pounds.

Table 1.—Range of coefficients in an equation of K_{II} as a function of loading conditions.

$$K_{II} = A\frac{M}{bd^{3/2}} + B\frac{V}{bd^{1/2}} + C\frac{W}{bd^{-1/2}}$$

Orthotropic parameters		Coefficients		
β_1	β_2	A	B	C
0.75	3.0	−3.112	−0.657	0.057
1.5	3.0	−2.864	− .674	.060
1.5	4.25	−2.577	− .779	.060
.75	4.25	−2.728	− .769	.068
1.125	3.625	−2.790	− .723	.062

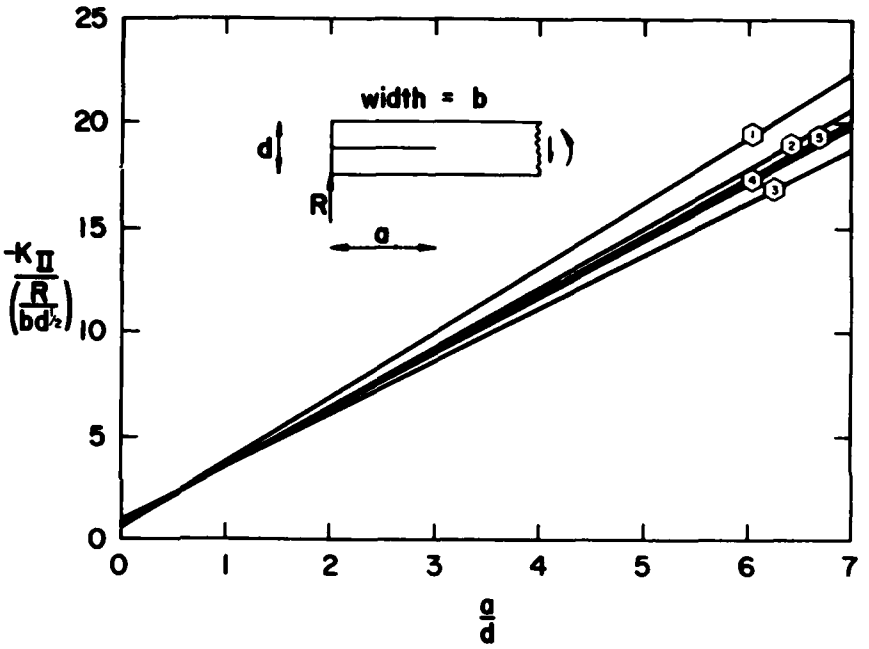

Figure 6.—Graph of dimensionless K_{II} as a function of relative crack length for an end-split beam under concentrated load.

(M 148 059)

"After the beams were tested, two block-shear specimens were cut from each of them in the neighborhood of the end of the saw kerfs and, subsequently, tested (1).

Presentation of Data

"The data obtained from the tests and some calculated values are given in table 2. The first column contains the beam number. Beams 3, 9, and 1(were omitted from the table because they were cross grained. Beam 15 was omitted because the shear failure was so gradual that it was not noted until the specimen was removed from the testing machine. The second column gives the length of the saw kerf measured from the position of the reaction toward the center of the beam, as shown in figure 7. The third column gives the distance from the end of the kerf to the position of the load. Column 4 gives the largest loads the beams withstood; and column 5 the first maximum load. These two loads are identical except for four beams. In these four tests the shear failures were not completely destructive; the beams failed and the load dropped, and, as the test proceeded, the load increased to a value greater than the first maximum.

"Column 6 of the table lists the value of the reaction at the first maximum load, and column 7 the shear stress computed by the formula

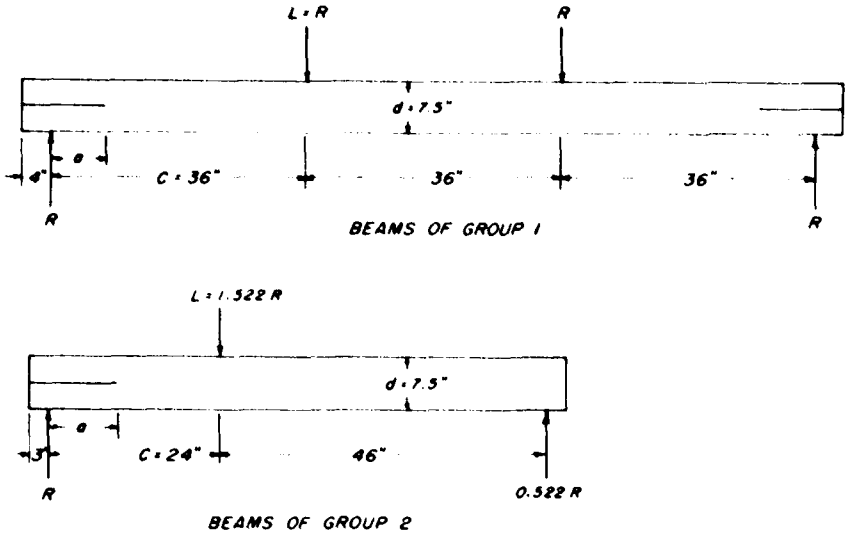

Figure 7.—Sketches of beams tested.
(M 148 083)

Table 2.—Pertinent data from the tests and some calculated values

Specimen No.	a	c-a	Maximum load	First maximum load	Reaction	τ_c	Results of block-shear tests		
							Specimen No. 1	Specimen No. 2	Average
(1)	(2)	(3)	(4)	(5)	(6)	(7)	(8)	(9)	(10)
	In.			*Lb.*			*Psi*		
				GROUP 1					
5	0	36	8,420	8,420	4,210	516	1,480	1,472	1,476
1	4	32	8,150	8,150	4,075	500	1,416	1,421	1,418
6	8	28	4,700	4,700	2,350	288	1,327	1,225	1,276
2	12	24	3,690	3,340	1,670	205	1,342	1,319	1,330
4	12	24	2,670	2,670	1,335	164	1,171	1,140	1,156
7	16	20	2,630	2,630	1,315	161	1,389	1,616	1,502
8	20	16	2,510	1,550	775	95	1,336	1,181	1,258
				GROUP 2					
11	5	19	7,170	7,170	4,710	578	1,519	1,526	1,522
13	5	19	5,240	5,240	3,440	428	1,435	1,302	1,368
16	9	15	3,225	3,225	2,120	260	1,352	1,222	1,287
19	9	15	3,090	3,090	2,030	249	1,277	1,130	1,204
12	13	11	3,000	2,500	1,640	201	1,339	1,363	1,351
'14	13	11	2,360	2,360	1,550	195	1,233	1,187	1,210
17	17	7	3,900	2,700	1,770	217	1,326	1,470	1,398
18	21	3	3,600	3,600	2,360	290	1,181	1,216	1,198

' Specimen 14 had a depth of 7.33 in.

$$\tau_c = \frac{3}{2}\frac{R}{bd}$$

Columns 8, 9, and 10 give the results of the block-shear tests made on specimens cut from the beam in the general location of the end of the saw kerf.

"The saw kerf in beam 5 was cut through the 4-inch overhang of the beam just to the position of the reaction. This kerf did not cause a shear failure. The beam failed at a modulus of rupture of 9,930 pounds per square inch, which is consistent with the average value of 11,200 given for coast-type Douglas-fir (10), taking into account the depth of the beam It would be expected that the presence of this kerf would not weaken the beam.

"The saw kerfs in beams 17 and 18 extended to within 7 and 3 inches of the position of the load. These two beams are not expected to satisfy the suggested equation because the ends of the kerfs are too close to the position of the load."

Comparison of Experiment with Theory

To analyze the experimental data, a theoretical equation similar to equation (3) is needed. (Eq. (3) is a suggested design equation, too general when comparing theory with experiment.) Using the orthotropic constants published (see (5)) for Douglas- fir (radial-longitudinal, RL) and a stress function boundary value collocation method (see appendices A and B), the equation for the mode II SIF was found to be

$$K_{II} = -2.785\frac{M}{bd^{3/2}} - 0.731\frac{V}{bd^{1/2}} + 0.0646\frac{W}{bd^{1/2}} \quad (4)$$

For a concentrated load case, equation (4) can be rewritten to

$$K_{II} = \left[-2.785\left(\frac{a}{d}\right) - 0.731\right]\frac{R}{bd^{1/2}} \quad (5)$$

where

K_{II} is the sliding mode SIF
a is crack length (column 2, table 2)
d is beam depth (7.5 in.)
b is beam width (1.62 in.)
R is reaction at support (column 6, table 2).

Using the experimental data and the theoretical equation (5), values of K_{II_c} were calculated for 12 beams (beams 5, 17, and 18 were not considered because of reasons noted earlier) and are listed in table C1. Because group 1 beams had two end splits and group 2 beams had only one, some adjustment between the two groups had to be made to obtain an average critical SIF $\overline{K}_{II_c}$ for a beam with only one end split. This adjustment is explained in appendix C. From the data of the 12 beams and statistical calculations, $\overline{K}_{II_c}$ was found to be 2,035 psi $\sqrt{}$ in. with a coefficient of variation (COV) = 15 percent, for a beam with one end split. This compares to the value

obtained by Barrett and Foschi (2) for western hemlock of 2,107 psi $\sqrt{\text{in.}}$. Figure 8 graphs $\frac{3}{2}\frac{R}{bd}$ versus $\frac{a}{d}$ using equation (5) ($w = 0$) and $\overline{K}_{IIc} = 2{,}035$ and 1,865 psi $\sqrt{\text{in.}}$ for single and double end-split beams, respectively. Also plotted in figure 8 are the experimental data showing the excellent agreement between experiment and theory. If the generalized species equation (3) is used instead of equation (4) with the test data, the $\overline{K}_{IIc}$ would be calculated to be about ½ percent higher.

Conclusions

1. Boundary value collocation can be used to accurately calculate the shear mode SIF in orthotropic wood beams.
2. Using superposition principles, one single equation can be written to calculate K_{II} for an end-split beam for either concentrated or uniform load cases.
3. Complex loadings can be handled by superposition of K_{II}'s.
4. The effect of different orthotropic parameters on the simplified equation is small enough so that one equation can be used for a majority of structural wood species.
5. Using the BVC method and species specific coefficients in the simplified equation, $\overline{K}_{IIc}$ for a species can be determined experimentally.
6. Douglas-fir $\overline{K}_{IIc}$ in the RL system was determined to be 2,035 psi $\sqrt{\text{in.}}$ at a moisture content of 11 percent.
7. A proposed simple failure equation for end-split beams is

$$K_{IIc} \leq -2.8\frac{M}{bd^{3/2}} - 0.72\frac{V}{bd^{1/2}} + 0.06\frac{W}{bd^{1/2}}$$

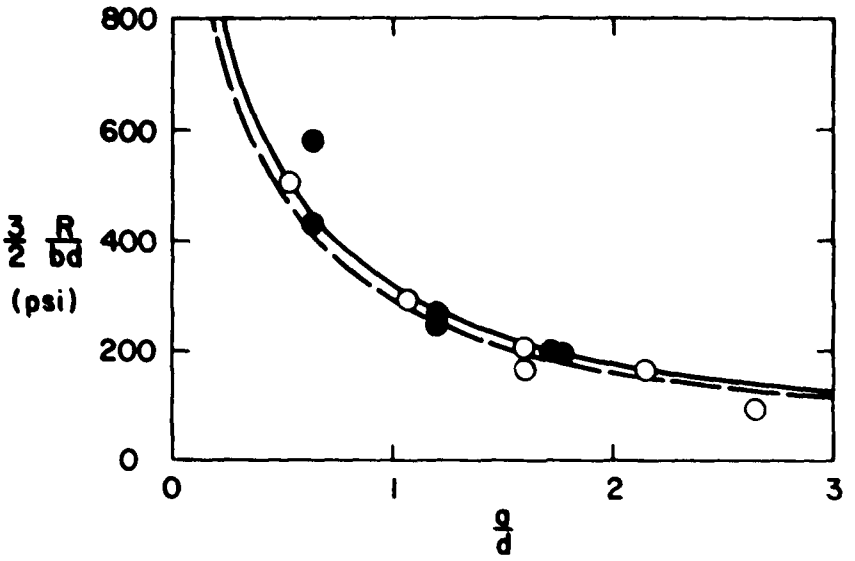

Figure 8.—Comparison of experimental data with theory, for end-split beams under concentrated loads (•—single-end split, o--double-end split).
(M 148 060)

U.S. Forest Products Laboratory.

Strength of wood beams with end splits, by J. F. Murphy, Madison, Wis., FPL., 1979 12 p. (USDA For. Serv. Res. Pap. FPL 347).

A quantitative measure of the effect of end splits on the strength of wood beams is useful in the grading for such beams.

This report presents a method of analysis for determining crack propagation loads on wood beams with end splits. A simple failure equation for end-split beams is also proposed.

U.S. Forest Products Laboratory.

Strength of wood beams with end splits, by J. F. Murphy, Madison, Wis., FPL., 1979 12 p. (USDA For. Serv. Res. Pap. FPL 347).

A quantitative measure of the effect of end splits on the strength of wood beams is useful in the grading for such beams.

This report presents a method of analysis for determining crack propagation loads on wood beams with end splits. A simple failure equation for end-split beams is also proposed.

U.S. Forest Products Laboratory.

Strength of wood beams with end splits, by J. F. Murphy, Madison, Wis., FPL., 1979 12 p. (USDA For. Serv. Res. Pap. FPL 347).

A quantitative measure of the effect of end splits on the strength of wood beams is useful in the grading for such beams.

This report presents a method of analysis for determining crack propagation loads on wood beams with end splits. A simple failure equation for end-split beams is also proposed.

U.S. Forest Products Laboratory.

Strength of wood beams with end splits, by J. F. Murphy, Madison, Wis., FPL., 1979 12 p. (USDA For. Serv. Res. Pap. FPL 347).

A quantitative measure of the effect of end splits on the strength of wood beams is useful in the grading for such beams.

This report presents a method of analysis for determining crack propagation loads on wood beams with end splits. A simple failure equation for end-split beams is also proposed.

Literature Cited

1. American Society for Testing and Materials.
   1949. Shear parallel to grain. ASTM Stand. D-143-49.

2. Barrett, J. D., and R. O. Foschi.
   1977. Mode II stress-intensity factors for cracked wood beams. Eng. Fract. Mech. 9(2):371-378.

3. Bowie, O. L.
   1973. Solutions of plane crack problems by mapping techniques. Ch. 1 *In* Mechanics of Fracture 1-Methods of Analysis and Solutions of Crack Problems. Noordhoff Int. Publ. 1-55.

4. Bury, K. V.
   1975. Statistical models in applied science. J. Wiley and Sons, Inc.

5. Forest Products Laboratory.
   1974. Wood handbook: Wood as an engineering material. U.S. Dep. of Agric., For. Serv., Agric. Handb. No. 72, rev.

6. Hogg, R. U., and A. T. Craig.
   1970. Introduction to mathematical statistics. Macmillan Co.

7. Isaacson, E., and H. B. Keller.
   1966. Analysis of numerical methods. J. Wiley and Sons, Inc.

8. Johnson, J. A.
   1973. Crack initiation in wood plates. Wood Sci. 6(2):151-158.

9. Lekhnitskii, S. G.
   1963. Theory of elasticity of an anisotropic body. Holden-Day, Inc.

10. Markwardt, L. J., and T. R. C. Wilson.
    1935. Strength and related properties of woods grown in the United States. U.S. Dep. of Agric., Tech. Bull. No. 479. Sept.

11. Muskhelishvili, N. I.
    1953. Some basic problems of mathematical theory of elasticity. P. Noordhoff and Co.

12. Rao, C. R.
    1965. Linear statistical inference and its application. J. Wiley and Sons, Inc.

13. Savin, G. N.
    1961. Stress concentration around holes. Pergammon Press.

14. Schniewind, A. P., and J. C. Centeno.
    1973. Fracture toughness and duration of load factor I. Six principal systems of crack propagation and the duration factor for cracks propagation parallel to grain. Wood and Fiber 5(2):152-159.

15. Sih, G. C., P. C. Paris, and G. R. Irwin.
    1965. On cracks in rectilinearly anisotropic bodies. Int. J. Fract. Mech. 1:189-203.

Appendix A

Formulation of the Complex Series Stress Functions for Cracked Orthotropic Bodies

Sih et al. (15) have given a general complex series stress function for a cracked rectilinearly anisotropic body. These functions simplify when the crack is parallel to a material axis. Leading up to these functions consider first an orthotropic body with a crack coincident with the negative x-axis (fig. A1) and a material axis.

The equilibrium equations (no body forces):

$$\frac{\partial \sigma_x}{\partial x} + \frac{\partial \tau_{xy}}{\partial y} = 0 \qquad \frac{\partial \sigma_y}{\partial y} + \frac{\partial \tau_{xy}}{\partial x} = 0$$

and compatibility equation:

$$\frac{\partial^2 \varepsilon_x}{\partial y^2} + \frac{\partial^2 \varepsilon_y}{\partial y^2} = \frac{\partial^2 \varepsilon_{xy}}{\partial x \partial y}$$

are combined into one field equation:

$$a_{22} \frac{\partial^4 U}{\partial x^4} + (2a_{12} + a_{66}) \frac{\partial^4 U}{\partial x^2 \partial y^2} + a_{11} \frac{\partial^4 U}{\partial y^4} = 0 \tag{A1}$$

using the following relations

$$\sigma_x = \frac{\partial^2 U}{\partial y^2} \quad \sigma_y = \frac{\partial^2 U}{\partial x^2} \quad \tau_{xy} = -\frac{\partial^2 U}{\partial x \partial y}$$

$$\varepsilon_x = a_{11}\sigma_x + a_{12}\sigma_y$$

$$\varepsilon_y = a_{12}\sigma_x + a_{22}\sigma_y$$

and

$$\varepsilon_{xy} = a_{66}\tau_{xy}$$

The coefficients a_{ij} are related to the engineering constants by

$$a_{11} = \frac{1}{E_x}, \; a_{12} = \frac{-\mu_{yx}}{E_y}, \; a_{22} = \frac{1}{E_y}, \; a_{66} = \frac{1}{G_{xy}} \tag{A2}$$

for plane stress and

$$a_{11} = \frac{1 - \mu_{zx}\mu_{xz}}{E_x}, \; a_{12} = \frac{-\mu_{yx} - \mu_{zx}\mu_{yz}}{E_y}$$

$$a_{22} = \frac{1 - \mu_{zy}\mu_{yz}}{E_y}, \; a_{66} = \frac{1}{G_{xy}}$$

for plane strain.

Specializing the rectilinearly anisotropic case of (3,9,11,13), the solution to the orthotropic field equation (A1) in terms of analytic functions F_j of complex variables z_j is

$$U(z_1,z_2) = 2\,\mathrm{Re}[F_1(z_1) + F_2(z_2)]$$

where

$$z_j = x + i\beta_j y = r(\cos\theta + i\beta_j \sin\theta) \qquad -\pi \le \theta \le \pi$$

where

$$i = \sqrt{-1}$$

Re means the real part of, and the β_j's satisfy the characteristic equation

$$a_{11}\beta_j^4 - (2a_{12} + a_{66})\beta_j^2 + a_{22} = 0. \tag{A3}$$

Introducing the notation

$$\frac{dF_j}{dz_j} = \phi_j(z_j) \text{ and } \frac{d\phi_j}{dz_j} = \phi_j'(z_j)$$

the expressions for stresses and displacements are

$$\begin{aligned} \sigma_x &= 2\,\mathrm{Re}[\mu_1^2\phi_0'(z_1) + \mu_2^2\psi_0'(z_2)] \\ \sigma_y &= 2\,\mathrm{Re}[\phi_0'(z_1) + \psi_0'(z_2)] \\ \tau_{xy} &= 2\,\mathrm{Im}[\mu_1\phi_0'(z_1) + \mu_2\psi_0'(z_2)] \\ u &= 2\,\mathrm{Re}[p_1\phi_0(z_1) + p_2\psi_0(z_2)] \\ v &= 2\,\mathrm{Im}[q_1\phi_0(z_1) + q_2\psi_0(z_2)] \end{aligned} \tag{A4}$$

where Im means the imaginary part of

$$p = a_{11}\mu^2 + a_{12}$$

and

$$q = a_{21}\mu + \frac{a_{22}}{\mu}$$

Figure A1 Coordinate system and positive directions for contour integration around a crack tip (from Sih et al. [2])

The resultant force and moment (about the origin) on arc length AB are (refer to fig. A1 for normal and tangential directions on the contour Γ enclosing area A_Γ)

$$\begin{aligned} X + iY &= -i\int_A^B (X_n + iY_n)\,ds = 2\,\mathrm{Im}[\phi_0 + \psi_0]_A^B \\ &\quad + 2\,\mathrm{Re}[\mu_1\phi_0 + \mu_2\psi_0]_A^B \end{aligned} \tag{A5}$$

$$\begin{aligned} M &= \int_A^B (xY_n - yX_n)\,ds = 2\,\mathrm{Re}[\mu_1\phi_1 + \mu_2\psi_1]_A^B \\ &\quad + 2x\,\mathrm{Re}[\phi_0 + \psi_0]_A^B \\ &\quad + 2y\,\mathrm{Im}[\mu_1\phi_0 + \mu_2\psi_0]_A^B \\ &\quad - 2\,\mathrm{Re}[\mu_1\phi_1 + \mu_2\psi_1]_A^B + xY - yX \end{aligned} \tag{A6}$$

where X_n, Y_n are the projections on the coordinate axes of the forces acting on the contour Γ of the area A_Γ. For a crack coincident with the negative x axis the stress function close to the tip is (from Sih et al. [2])

$$\phi_0(z) = \frac{K}{\sqrt{2\pi}}\,z_1^{-\frac{1}{2}} + \cdots$$

where

$$z_1 = x_1 + \mu_1 y_1$$

This function gives finite displacements and infinite stresses at the crack tip ($\sigma_{ij} \propto r^{-\frac{1}{2}}$) and satisfies the field equation.

To satisfy the stress free condition on the crack surfaces requires

$$a_{2n} = \frac{\delta_n}{\delta_2}\,a_{1n}\,b_{2n} = b_{1n}, \quad n \text{ odd}$$

and

$$a_{2n} = a_{1n}\,b_{2n} = \frac{\delta_n}{\delta_2}\,b_{1n}, \quad n \text{ even}$$

The remaining coefficients (a_{1n}'s and b_{1n}'s) of the complex series stress function are obtained using a boundary value collocation method as described in appendix B.

The leading coefficient λ_{11} is related to the SIF's K_I, K_{II} by the relationship:

$$K_I = - a_{11} \sqrt{8\pi} \left(\frac{\beta_1 - \beta_2}{\beta_2}\right)$$

and

$$K_{II} = b_{11} \sqrt{8\pi} \, (\beta_1 - \beta_2).$$

Appendix B

Boundary Value Collocation and Numerical Method

In a boundary value collocation method (or point matching) the form of the solution satisfies the governing field equation everywhere in the interior of the body. The constants or coefficients appearing in the solution are obtained by evaluating the solution at a finite number of boundary points. Infinite series solutions are first truncated such that the number of unknown constants are at most equal to the number of boundary conditions to be evaluated. If more boundary conditions are specified than unknown coefficients, the unknowns can be solved for in a least-squares sense. Solving in a least-squares sense has the advantage of reducing off-point errors, though making the linear system of equations more ill-conditioned.

To apply the boundary value collocation method to a cracked orthotropic body, the complex stress function (see appendix A) and associated integrals are approximated by:

$$\phi_j'(z_j) \cong \sum_{n=1}^{M} \lambda_{jn} (z_j)^{\frac{n}{2} - 1}$$

$$\phi_j'(z_j) \cong \sum_{n=1}^{M} \frac{\lambda_{jn}}{\frac{n}{2}} (z_j)^{\frac{n}{2}}$$

and

$$F_j(z_j) \cong \sum_{n=1}^{M} \frac{\lambda_{jn}}{\frac{n}{2}\left(\frac{n}{2} + 1\right)} (z_j)^{\frac{n}{2} + 1}$$

These functions are now used (according to eq. (A4) to (A6) to specify stress, displacement, or resultants at a discrete number of boundary points, and the resulting linear equations can be written in matrix notation as

$$A X = B$$

where X contains M (not to be confused with moment M in text and appendix A) unknown complex constants λ_{jn}, matrix A contains functions of position and β_j's, and B contains N corresponding boundary stress, displacement, or resultant values. For the orthotropic crack-alined case the $Re[\lambda_{jn}] = a_{jn}$ corresponds to symmetric (about the x-axis) in-plane loading only, while $Im[\lambda_{jn}] = b_{jn}$ corresponds to skew-symmetric in-plane loading. Thus the general case is really the sum of two separate problems:

$$A \, Re[\lambda] = B_{SYM} \text{ and } A \, Im[\lambda] = B_{SKEW}$$

which are solved separately. Each case automatically satisfies appropriate stress derivatives ahead of the crack and because of geometric symmetry only the region $y > 0$ has to be considered. The procedure used will be given and then the rationale for each procedural step will be explained later.

Begin first with an overspecified system

$$AX = B,$$

where

A is an N X M known matrix
X is an M X 1 unknown column vector

and

B is an N X 1 known column vector

and

$$M \leq N.$$

First postmultiply A by an (M × M) diagonal matrix D to get

$$AD \, D^{-1} X = ADy = Cy = B \qquad \text{(B1)}$$

and premultiply C and B by the transpose of C knowing that

$$C^TCy = C^TB.$$

The square (M × M) matrix C^TC is equal to T^TT where T is an upper triangular (M × M) and is obtained by triangular reduction by an orthonormal matrix R such that

$$RA = \begin{pmatrix} T \\ 0 \end{pmatrix}$$

(see (12)). The matrix equation is now

$$T^TTy = C^TB$$

Taking the inverse of the left side gives the matrix equation for the unknown column vector

$$X = DT^{-1}T^{-T}C^TB$$

Both the matrices X and B can be generalized to K columns so that a K number of problems (with the same orthotropy and geometry and different loadings) can be solved simultaneously.

The matrix A is scaled by postmultiplying it by the diagonal matrix D in equation (B1) to achieve greater accuracy in the solution than when it is not scaled. The resulting scaled matrix is required to have column Euclidean norms approximately equal to unity and the diagonal elements of D are powers of two to avoid introducing computer roundoff errors. Finding T from A directly by triangular reduction by an orthonormal matrix is believed to be numerically more stable than by Gram-Schmidt triangular reduction (12) and requires less computation than using Cholesky factorization of C^TC into T^TT. Finally then, the only matrix inversion is the simple inversion of a triangular matrix (T). It was found that scaling and triangular reduction increased the accuracy of X and in some instances (M large) gave answers when elimination methods, double precision, and iteration improvement did not.

Appendix C

Statistics

Using the experimental data from table 2 and the theoretical equation (4), table C1 is constructed.

Since in group 1 the weaker of two K_{II} was measured, the data cannot be lumped together without some algebraic adjustment first. Assume that for a single set of conditions (one split, etc.) K_{II_c} is normally distributed $N(\mu_1, \sigma_1^2)$; assume also that for two splits the measured K_{II_c} is the lower value of two independent K_{II_c}, each having the same distribution; then, the probability density function (p.d.f.) of this measured K_{II_c} is (using series reliability (4))

$$g_2(y; \mu_1, \sigma_1) = 2[1-F_N(y; \mu_1, \sigma_1)]\, f_N(y; \mu_1, \sigma_1) \qquad \text{(C1)}$$

where

$$f_N(x; \mu_1, \sigma_1) = \frac{1}{\sigma_1\sqrt{2\pi}}\, e^{-\frac{1}{2}\left|\frac{x-\mu_1}{\sigma_1}\right|^2}$$

and

$$F_N(x; \mu_1, \sigma_1) = \int_{-\infty}^{x} f_N(y; \mu_1, \sigma_1)dy$$

Using the method of maximum likelihood (6), we write a likelihood function L as

$$L(\mu_1, \sigma_1; x_1, x_2, \ldots, x_6, y_1, y_2, \ldots, y_6) = \prod_{i=1}^{6} g_2(y_i; \mu_1, \sigma_1)\, f_N(x_i; \mu_1, \sigma_1)$$

where x_i are observed values from group 2 (column 3, table C1) and y_i are observed values from group 1 (column 4, table C1). The maximum likelihood estimates for μ_1 and σ_1 are found such that

$$\frac{\partial L}{\partial \mu_1} = 0 \text{ and } \frac{\partial L}{\partial \sigma_1^2} = 0.$$

This was done with the data from table C1 resulting in

$$\hat{\mu}_1 = 2{,}035 \text{ psi}\sqrt{\text{in.}}$$

and

$$\hat{\sigma}_1 = 301 \text{ psi}\sqrt{\text{in.}}.$$

These are estimates of the mean and standard deviation for a single-split beam.

The expected value for the group 1 set is

$$\mu_2 = \int_{-\infty}^{\infty} x\, g_2(x)dx \qquad \text{(C2)}$$

With a change of variables equation (C2) becomes

$$\mu_2 = \int_{-\infty}^{\infty}(x\sigma_1 + \mu_1)\, 2[1 - \Phi(x)]\, \phi(x)dx \qquad \text{(C3)}$$

where $\phi(x)$ is the p.d.f. and $\Phi(x)$ is the c.d.f. (cumulative distribution function) of the standardized normal distribution. Equation (C3) can be evaluated:

$$\mu_2 = \sigma_1 \int_{-\infty}^{\infty} x2[1 - \Phi(x)]\, \phi(x)dx + \mu_1[1 - \Phi(x)]^2 \Big|_{-\infty}^{\infty}$$

$$\mu_2 = C\sigma_1 + \mu_1 \qquad \text{(C4)}$$

The variance is

$$\sigma_2^2 = \int_{-\infty}^{\infty} x^2 g_2(x)dx - \mu_2^2$$

but

$$\int_{-\infty}^{\infty} x^2 g_2(x)dx = \int_{-\infty}^{\infty} (x\sigma_1 + \mu_1)^2\, 2[1 - \Phi(x)]\, \phi(x)dx$$

$$= \sigma_1^2 \left| \int_{-\infty}^{\infty} x^2\, \phi(x)dx + \int_{-\infty}^{\infty} x^2 2[1/2 - \Phi(x)]\phi(x)dx \right|$$

$$+ 2\mu_1\sigma_1 \int_{-\infty}^{\infty} x2[1 - \Phi(x)]\, \phi(x)dx + \mu_1^2 \int_{-\infty}^{\infty} 2[1 - \Phi(x)]\phi(x)dx$$

$$= \sigma_1^2[1 + 0] + 2\mu_1\sigma_1 C + \mu_1^2$$

resulting in

$$\sigma_2^2 = \sigma_1^2 + 2\mu_1\sigma_1 C + \mu_1^2 - \mu_2^2$$

Using equation (C4) gives

$$\sigma_2^2 = [1 - C^2]\sigma_1^2 \qquad \text{(C5)}$$

The constant C was calculated by numerical integration to be -0.5642 yielding:

$$\hat{\mu}_2 = \hat{\mu}_1 - 0.5642\hat{\sigma}_1 = 1{,}865 \text{ psi} \sqrt{\text{in.}}$$

and

$$\hat{\sigma}_2 = 0.8256\hat{\sigma}_1 = 249 \text{ psi} \sqrt{\text{in.}} \qquad \text{(C6)}$$

Therefore, if a beam has one split which would always fail first, μ_1 and σ_1 would describe the mean and variance of K_{IIc}, and if a beam has two splits (each with the same K_{II}), μ_2 and σ_2 would describe the mean and variance of the observed K_{IIc}.

Table C1.—Computed K_{IIc} from experiments

Specimen number	K_{IIc}, x_i	K_{IIc}, y_i	Specimen number	K_{IIc}, x_i	K_{IIc}, y_i
	GROUP 1			GROUP 2	
1	—	2,036	11	2,747	—
6	—	1,961	13	2,006	—
2	—	1,952	16	1,946	—
4	—	1,561	19	1,864	—
7	—	1,978	12	2,055	—
8	—	1,425	14	2,004	—